NPS63-84-005

NAVAL POSTGRADUATE SCHOOL

Monterey, California

SOME ASPECTS OF POST-FRONTAL CONVECTIVE AREAS
ALONG THE WEST COAST OF THE UNITED STATES

Francis J. Winninghoff
Russell L. Elsberry

December 1983

Final Report for Period October 1982 - September 1983

Approved for public release; distribution unlimited.

Prepared for: National Aeronautics and Space Administration
Washington, DC 20546

Naval Environmental Prediction Research Facility
Monterey, CA 93943

NAVAL POSTGRADUATE SCHOOL
Monterey, California 93943

Commodore R. H. Shumaker
Superintendent

David A. Schrady
Provost

The research reported herein has been carried out under the sponsorship of two agencies: National Aeronautics and Space Administration under Contract 623-GW-86B and the Naval Environmental Prediction Research Facility, under Program Element 62759N.

This reported was prepared by:

REPORT DOCUMENTATION PAGE

READ INSTRUCTIONS BEFORE COMPLETING FORM

1. REPORT NUMBER: NPS63-84-005	2. GOVT ACCESSION NO.
3. RECIPIENT'S CATALOG NUMBER	
4. TITLE (and Subtitle): Some Aspects of Post-frontal Convective Areas along the West Coast of the United States	5. TYPE OF REPORT & PERIOD COVERED: Final Report October 1982-September 1983
6. PERFORMING ORG. REPORT NUMBER	
7. AUTHOR(s): Francis J. Winninghoff, Russell L. Elsberry	8. CONTRACT OR GRANT NUMBER(s): NASA 623-GW-86B
9. PERFORMING ORGANIZATION NAME AND ADDRESS: Department of Meteorology, Naval Postgraduate School, Monterey, CA 93943	10. PROGRAM ELEMENT, PROJECT, TASK AREA & WORK UNIT NUMBERS: NEPRF 62759N Project WF59-551
11. CONTROLLING OFFICE NAME AND ADDRESS	12. REPORT DATE: December 1983
	13. NUMBER OF PAGES: 38
14. MONITORING AGENCY NAME & ADDRESS (if different from Controlling Office)	15. SECURITY CLASS. (of this report): Unclassified
	15a. DECLASSIFICATION/DOWNGRADING SCHEDULE

16. DISTRIBUTION STATEMENT (of this Report)

Approved for public release; distribution unlimited.

17. DISTRIBUTION STATEMENT (of the abstract entered in Block 20, if different from Report)

18. SUPPLEMENTARY NOTES

19. KEY WORDS (Continue on reverse side if necessary and identify by block number)

Cumulus convection areas
Post-frontal convection
Latent heat parameterization
FGGE case study

20. ABSTRACT (Continue on reverse side if necessary and identify by block number)

The European Center for Medium-Range Weather Forecasts (ECMWF) Level III-b analyses are used to study cases of post-frontal convective areas that occurred off the West Coast of the United States. A five-year climatology suggests than an average of about 13 convective events occurs each winter, and that two of three cases are likely to have intense and well-organized convection. Five events that occurred during the First Special Observing Period of the First GARP Global Experiment are selected for detailed study.

DD FORM 1 JAN 73 1473 EDITION OF 1 NOV 65 IS OBSOLETE S/N 0102-014-6601

Unclassified

SECURITY CLASSIFICATION OF THIS PAGE (When Data Entered)

Associations are sought between the post-frontal convective areas and standard synoptic and dynamic variables. The convection appears to be closely tied to the position of the upper level cold trough. Cold advec aloft and low-level heating as the cold air streams over the warmer ocea contribute to maintenance of low static stability in the convective regi The feasibility of diagnosing the location of the convective regions is explored with diabatic and frictional parameterizations of the Naval Ope tional Global Atmospheric Prediction System (NOGAPS). Wind, temperature geopotential and moisture fields from the ECMWF are used to specify the large-scale forcing. The cumulus precipitation diagnosed by the NOGAPS agree surprisingly well with the post-frontal convective areas in these five cases.

List of Figures

ABSTRACT

The European Center for Medium-Range Weather Forecasts (ECMWF) Level III-b analyses are used to study cases of post-frontal convective areas that occurred off the West Coast of the United States. A five-year climatology suggests that an average of about 13 convective events occurs each winter, and that two of three cases are likely to have intense and well-organized convection. Five events that occurred during the First Special Observing Period of the First GARP Global Experiment are selected for detailed study. Associations are sought between the post-frontal convective areas and standard synoptic and dynamic variables. The convection appears to be closely tied to the position of the upper level cold trough. Cold advection aloft and low-level heating as the cold air streams over the warmer ocean contribute to maintenance of low static stability in the convective region. The feasibility of diagnosing the location of the convective regions is explored with diabatic and frictional parameterizations of the Naval Operational Global Atmospheric Prediction System (NOGAPS). Wind, temperature, geopotential and moisture fields from the ECMWF are used to specify the large-scale forcing. The cumulus precipitation diagnosed by the NOGAPS does agree surprisingly well with the post-frontal convective areas in these five cases.

1. Introduction

Much attention has been devoted in meteorology to the problem of forecasting maritime cyclogenesis off the eastern coasts of North America and Asia. Those regions with concentrated sea-surface temperature gradients experience destructive weather phenomena both on large scales and small scales. In the eastern parts of the oceans, the horizontal temperature gradients are usually less. Consequently, surface fronts are not as sharp and there is less severe local weather. Nevertheless, there are periods during the cold season when predominantly convective weather causes a troublesome forecast problem along the west coast of the United States. Following strong trough passages, convection intense enough to cause rain or hail showers with some thunder occurs within strong bursts of arctic or polar air over the relatively warm ocean. However, the intensity of these convective situations varies considerably. When the convection is very intense, it may produce rain over a large area well after the frontal passage, or tornadoes or waterspouts may be observed (as in Los Angeles on 1 March 1983). Monteverdi (1976) estimates that about 30% of all the precipitation at San Francisco originates under these conditions. These situations are often not well forecast by numerical forecast models, presumably because of the small horizontal scales involved, and the convective nature of the weather.

Among the notable achievements of dynamic meteorology since the 1930's has been the progress in understanding the mechanism responsible for extratropical cyclogenesis--namely, baroclinic instability. However, there are extratropical weather phenomena associated with somewhat smaller temporal and spatial scales that are not well forecast, even though the theory may be understood to some extent. For example, very rapid extratropical cyclone developments are often not well forecast, especially over the seas and near the east coasts of

Asia and North America (Sanders and Gyakum, 1980). Another maritime forecast problem is the prediction of polar lows. These are quite intense, small-scale cyclones that occasionally develop within very cold air masses passing over high latitude oceans from such cold source regions as Greenland, Siberia or Antarctica (see references in Sardie and Warner, 1983). There is very active research into the origin of these lows. Some authors suggest that baroclinic instability is the generating mechanism (Reed, 1979; Mullen, 1979, 1982), while others favor CISK (Rasmussen, 1979). Sandgathe (1982) used the Naval Operational Global Prediction System (NOGAPS) model to simulate small-scale oceanic cyclones under a very strong jet. He concluded that these systems are caused by baroclinic instability in which horizontal temperature gradients and associated vertical wind shear play the dominant role. The small-scale cyclones developing in weaker flow may also owe their growth to baroclinic instability if the static stability is sufficiently small, and this energy source may be supplemented in some cases by latent heat release. Inclusion of moisture, especially under conditions of small static stability, does shift the maximum growth rate to smaller scale disturbances in the linear baroclinic instability theory, whether the latent heat is added by convective clouds or large-scale precipitation (Staley and Gall, 1978; Lindzen, 1974; Mak, 1982).

There are many studies of convective-type phenomena using satellite information that indicate the varying degrees of organization of convective clouds. Locatelli, et al. (1982) have also incorporated radar and aircraft data in a detailed study of post-frontal convection that frequently leads to a situation that is analyzed as an "instant occlusion" of the front. Even though these convective patterns frequently appear in the post-frontal cold air, the presently operational numerical forecast models often encounter difficulty in forecasting the weather associated with these patterns.

The purpose of this study is to examine some of these post-frontal convective patterns occurring off the west coast of California using the state-of-the-art diabatics package in the NOGAPS model in a diagnostic mode. The European Center for Medium-Range Weather Forecasts (ECMWF) Level III-B analyses (Bjorheim, et al., 1982) during the Special Observing Period (SOP) of the First GARP Global Experiment (FGGE) are used, as these fields are likely to be the best available for some time. It is hoped that this study can lead to a better understanding of such phenomena and demonstrate the possibility of improved predictions of the post-frontal convective situations.

2. Data Classification

Surface, upper air charts and satellite pictures from five winters (1977-1978 through 1981-1982) were examined to isolate and classify cases of interest. The winter of 1978-79 is of special interest since that was the period of the very intense FGGE observing period. The procedure was to first examine 500 mb maps for cases of strong trough passages at San Francisco (SFO), which is representative of the central coastal region of California. A strong 500 mb trough is defined as: a minimum temperature of $-20^{\circ}C$ or less; heights less than 5700 m; and wind speeds greater than 25 m/sec. With these synoptic conditions, patterns of rising motion and/or convective instability are expected from November to April. The sample was further stratified by use of the surface maps. Interest was concentrated on those cases in which surface reports continued to indicate general showery weather or rain for a day or two after the frontal passage. The criteria above were applied fairly loosely to ensure inclusion of as many cases as possible. Based on this procedure, 64 possible cases were identified off the California and Oregon coasts during the five winters. Many more cases could have been included if the domain had been extended into the Gulf of Alaska.

Next, the visual and infrared (IR) satellite pictures in the Naval Postgraduate School archives were examined. Several patterns did emerge that appeared to be related to the observed weather. The first (I) pattern (Fig. 1a) is widely-scattered, cellular convection following a frontal band. Over land this pattern may be totally obscured by the topography. Although there may be quite heavy or moderate rain in the frontal band, there is at most scattered, light showers in the cellular convection following the front. This open cell pattern is reminiscent of Benard convection. In the second (II) pattern (Fig. 1b), there is greater organization of convective activity behind the front. There is a certain degree of bandedness in the clouds. Although showers are more numerous in this situation, the total rainfall may still be only of 2.5 mm at most stations. There are three further stages in the convective organization: (III), the band in (II) takes the form of a patch of clouds; (IV), the patch becomes quite solid in appearance; and (V), the solid cluster takes on a definite comma shape. These five patterns (I-V) are schematically illustrated in Fig. 1a-e. In the case of the comma pattern (V), extensive thunderstorms may occur with general rain, which may in some cases exceed the rainfall associated with the original frontal passage. Polar lows, at least in the sense discussed by the authors mentioned in the Introduction, were not observed in this region during the SOP. When there was a separate non-frontal surface low, it was associated directly with the main upper level trough or cut-off low.

Using these five patterns as a basis, the 64 cases have been classified into three general categories of convective activity: light, moderate and intense. The light category is pattern (I). The moderate category includes patterns (II) and (III), and the intense category includes patterns (IV) and (V). The tabulation of these cases during each winter (see Appendix A)

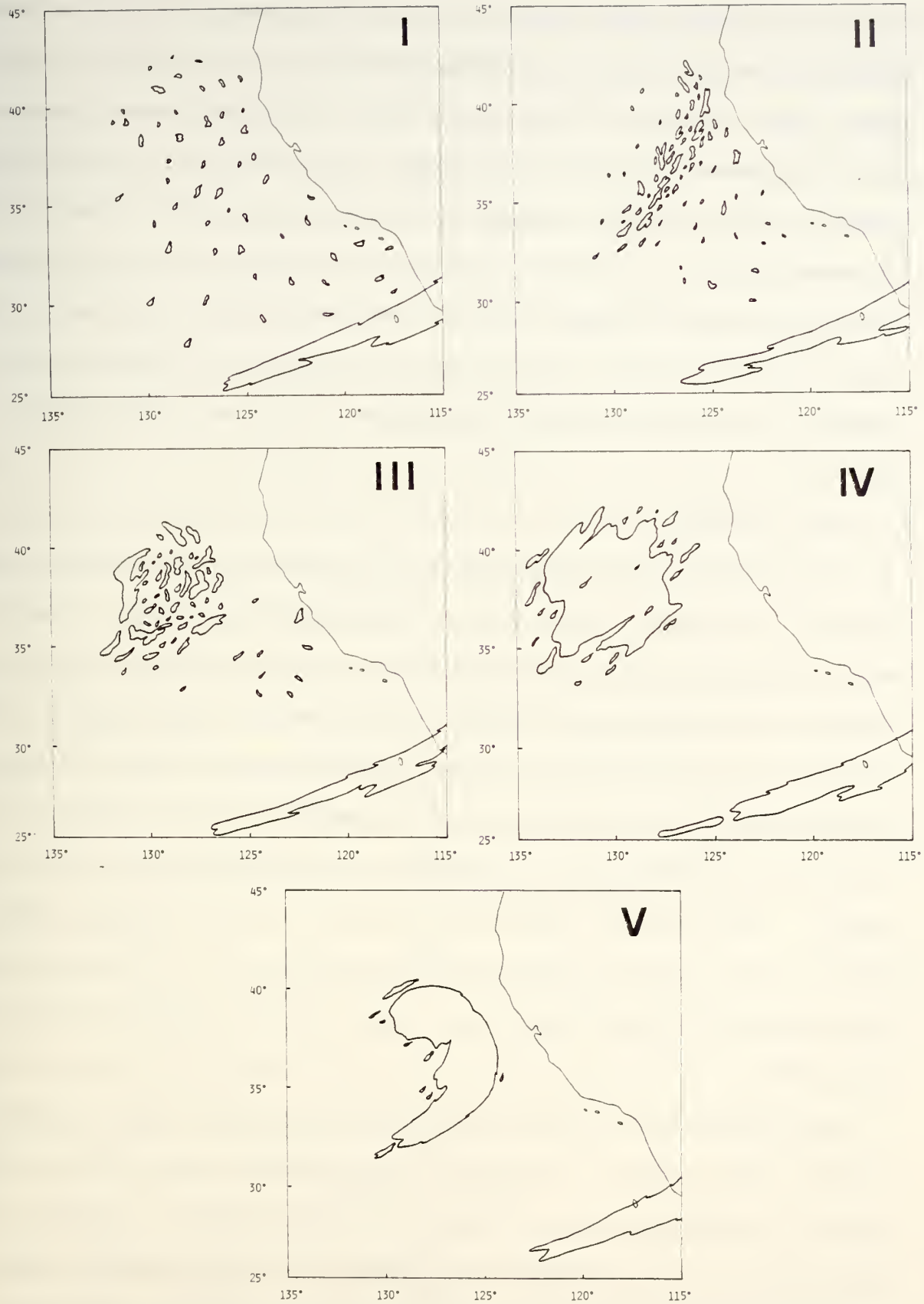

Figure 1. Schematic representation of post-frontal convective patterns. See text for description of stages I-V.

indicates that these situations occur fairly frequently. In the five winters studied, an average of 12.8 cases were identified off the California and Oregon coasts, of which 1.8 cases each winter were in the intense category. Thus, these events are common enough that forecasters need to be concerned. There also appears to be a tendency for a grouping of cases. When this grouping occurs, there is significant weather for a number of days. The convective post-frontal features then contribute to a sequence of rainstorms with nearly a daily cycle. Correctly forecasting the continuation, or the end, of a sequence of such events is very important for public and civil aviation interests.

3. Analysis methods

It is possible to discuss qualitatively phenomena such as these clusters and commas in terms of short waves, convectively-driven storms, etc. With the normal data coverage over areas such as the eastern Pacific Ocean, it is nearly hopeless to attempt more quantitative discussion. During the SOP of FGGE in the winter of 1978-1979, many special observations were incorporated into the ECMWF Level III-B analyses. It was hoped that the data coverage during the FGGE period (ECMWF, Vol. 1, Dec 1978 - Feb 1979) would allow quantitative studies. Unfortunately, there were no Intense category situations during the SOP, but there were four Moderate events (see Table I): 4-6 Jan, 15-17 Jan, 30-31 Jan and 20-22 Feb 1979. Also, a light intensity event occurred on 17-19 Dec 1978.

The ECMWF analyses include the following variables: surface pressure, heights, wind components, temperature, vertical motion and relative humidity at 100, 150, 200, 250, 300, 400, 500, 700, 850 and 1000 mb. A series of charts at 12-h or 6-h intervals was prepared for each of the five cases. The study area extended from 146°W to 100°W and from 18.75°N to 60°N with a

resolution of 1.875 degrees latitude and longitude. The approximate area of deep convection indicated on the IR pictures was superposed on each chart.

The first charts examined were the surface pressure and the 500 mb height fields. Since it is of interest to understand what type of physical "instability" plays a more dominant role in the formation and maintenance of these convective areas, patterns of vertical motion, static stability and moisture were also examined. Quasi-geostrophic reasoning suggests that the convection patterns might be associated with spatial patterns of the horizontal temperature advection and with vertical shear in the vorticity advection. Vorticity fields at three levels were mapped to determine if relationships exist between the convective cloud areas and the advection of vorticity. Temperature advection at 850, 700 and 500 mb and moisture advection at 850 mb and 700 mb were also examined. Of course, large-scale vertical motion does result from more than positive vorticity advection shear or the Laplacian of temperature advection. The ECMWF omega fields are derived using a normal mode method, and are approximately equivalent to the omegas from a more complete form of the omega equation containing nine forcing terms (Krishnamurti, 1968). These ECMWF omega fields at 850, 700 and 500 mb were also examined for any coherence with the convective patterns.

The spatial scale of the convective areas being considered in this work is not clearly "large-scale". The radius of deformation for mid-latitudes is typically greater than 1000 km (using a value for internal gravity waves), which implies a wavelength greater than 6000 km. The convective areas considered here have a much shorter scale than this. Because the wind fields tend to dominate the mass fields on these spatial scales, the kinematic vertical velocities are probably more appropriate than the quasi-geostrophic or normal mode omega values. The kinematic vertical motions are usually

difficult to compute accurately due to errors in the winds. Therefore, the ECMWF omegas at the top and bottom of the column were used to bound the kinematic omegas calculated from the wind fields. The kinematic omega fields were mapped at 850, 700 and 500 mb. Finally, stability values ($d\theta/dp$) were mapped for the layers 1000-850 mb, 850-700 mb and 700-500 mb.

The ECMWF data were also used as input into the heating package of the NOGAPS model. This model was based on the general circulation model developed over many years at UCLA under the direction of Prof. A. Arakawa. The heating package is normally run in conjunction with the integration of the forecast model using time-dependent values of boundary layer depth, and wind temperature and moisture jumps at the top of the layer. The planetary boundary layer parameterization also requires ocean temperatures to calculate fluxes. These temperatures were provided from the Fleet Numerical Oceanography Center's operational daily analyses. A budget of heat and moisture is normally used in the model to estimate ground temperature. In this diagnostic application of the heating package, the land areas were passive, i.e. the surface temperature is set at the same value as the lowest level in the ECMWF data. Heights of the land surface above sea level were set to zero, as the principal area of interest was the oceanic region. Since some of the variables mentioned above are not available, the frictional and diabatic package is provided with the data from each case and at least nine iterations (complete cycles through the heating package at a given time level) are used to allow the boundary layer thickness and inversion jumps to develop. One of the most interesting products is cumulus scale precipitation. These fields were superposed on the convective areas for the five cases. Also fields of evaporation computed from the NOGAPS boundary layer were prepared at each time level of the five cases to determine moisture source regions. A more detailed description of the

diagnostic application of the NOGAPS PBL and convective parameterization with the ECMWF analyses is contained in a forthcoming NPS report by C.-S. Liou and R. L. Elsberry.

4. Results

Since the total number of charts and satellite pictures is quite large, detailed accounts of each case will not be presented. One of the five cases during the SOP will be presented in some detail. The remaining four cases will be discussed only in terms of the significant variables described in the first case.

a. Case Study 1

The convective region that occurred from 17-19 Dec 1978 is presented to illustrate the evolution and relationships with synoptic and NOGAPS variables. This case has been labeled a category I or Light case and the reader may readily verify in Fig. 2 that the post-frontal convection remained patchy, although it was very distinct throughout the period. Beginning at 0315GMT 17 Dec 1979 (Fig. 2a), a large amount of cloudiness that originated on the ITCZ was streaming into the southern tip of California. A frontal band extended southwestward from northern California. The patchy area of convection was centered near 43°N, 134°W. By 1545GMT 17 Dec (Fig. 2b), the frontal band, which was now into central California, began to merge with the large band of tropical origin, and the convective patch was centered near 40°N, 130°W. Proceeding to 0345GMT 18 Dec (Fig. 2c), the patch was now centered west of San Francisco at about 127°W, whereas the front had merged into the band of cloudiness over southern California. During the 18th (Fig. 2d), the patch gradually moved into the coast and the merged tropical-frontal cloud band moved eastward. By 1545GMT 19 Dec (not shown), the patch had moved into the band and dissipated.

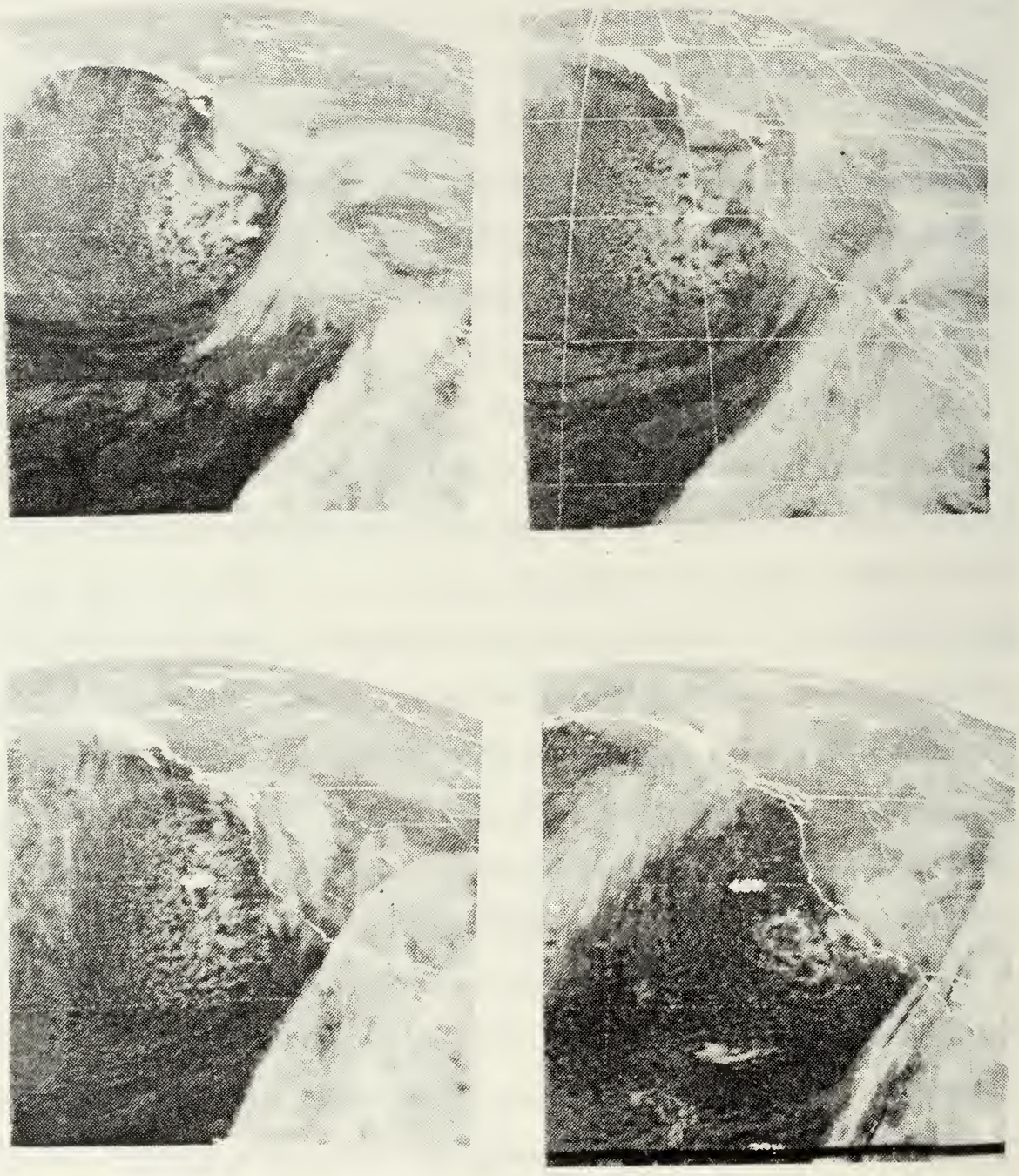

Figure 2. Infrared imagery from GOES West on: (a) 0315GMT 17 Dec 1978; (b) 1545GMT 17 Dec 1978; (c) 0345GMT 18 Dec; and (d) 0045GMT 19 Dec.

This case was not a major rainfall event in California except near the southern border. For example, SFO registered 0.59" on the 17th and an additional 0.14" on the 18th, whereas the Los Angeles Civic Center received 0.14" on the 16th, 0.35" on the 17th, 0.84" on the 18th and 0.10" on the 19th. In San Diego, however, 0.14" fell on the 16th and 1.32" fell on the 17th under the influence of the subtropical cloudiness. Furthermore, 0.38" was registered on the 18th and 0.27" on the 19th.

The surface low at 49°N, 129°W on the 00GMT 17 Dec analysis from ECMWF (Fig. 3a) was moderately deep at 988 mb. The primary low took a normal eastward path and moved into the coast by 00GMT 18 Dec (Fig. 3b) and weakened to 1000 mb. Then it moved rapidly southeastward to a position over Utah by 00GMT 19 Dec (Fig. 3c) and into Nebraska by 12 h later (not shown). On the larger scale ECMWF analyses, a subtropical trough centered at 128°-129°W at 00GMT 17 Dec gradually shifted eastward and combined with the frontal trough. In this case there was no separate surface low trailing the system off the California coast, which is a departure from the remaining four cases to be discussed below. Superposed on the maps is the approximate area of patchy convection as shown on the IR satellite pictures. The patch can be followed from 00GMT 17 Dec to 00GMT 19 Dec as it moved southeastward to the coast. On the whole it tended to remain southwest of the surface low in the NNW to NW flow.

The corresponding 500 mb maps from the ECMWF during the period are shown in Figs. 4a-c. A moderate open-wave trough was centered near 135°W at 00GMT 17 Dec, with its strongest gradients near 37°-41°N. This trough moved southeastward to the coast by 00GMT 19 Dec, with the strongest geostrophic winds at the later time located at 30°N-32°N. The patchy convection in this case remained just to the east of the trough axis until 00GMT 18 Dec, when it was located on the axis of the trough. The corresponding relative vorticity

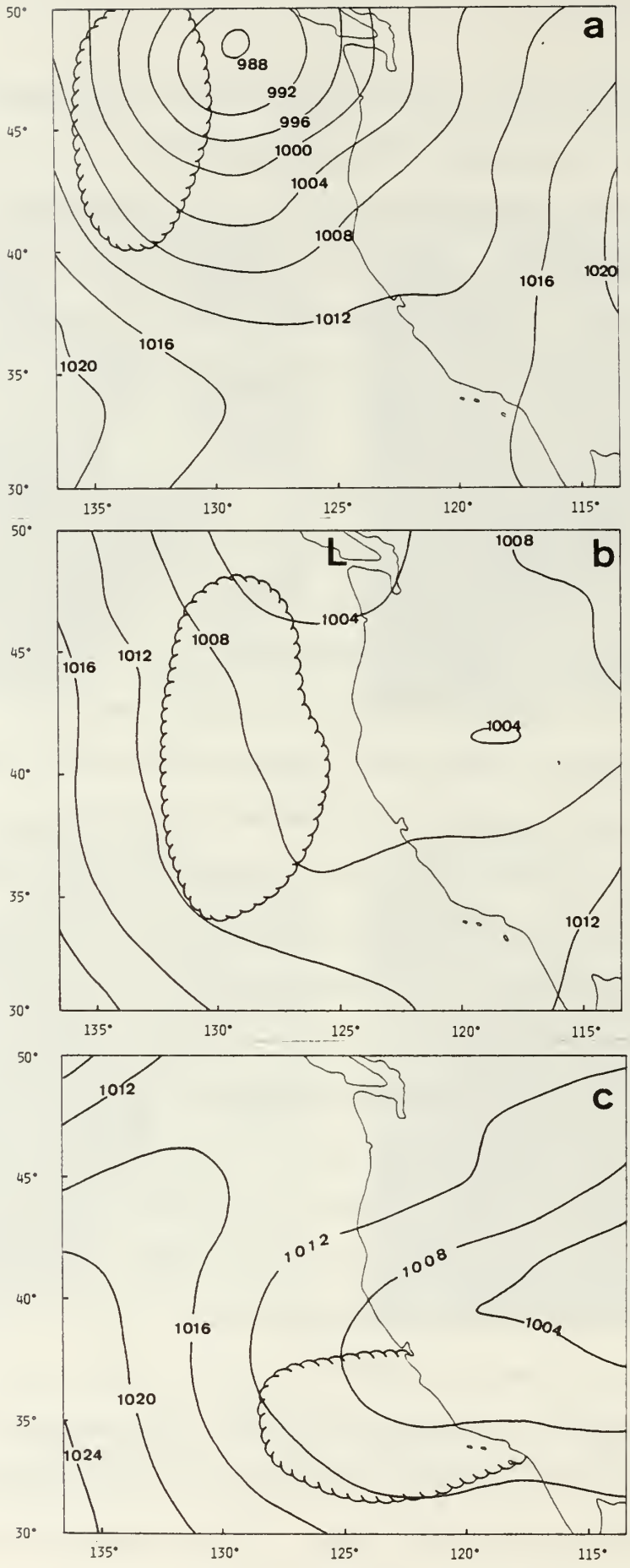

Figure 3. Surface pressure and patchy convective area (scalloped) on: (a) 00GMT 17 Dec 1978; (b) 00GMT 18 Dec; and (c) 00GMT 19 Dec.

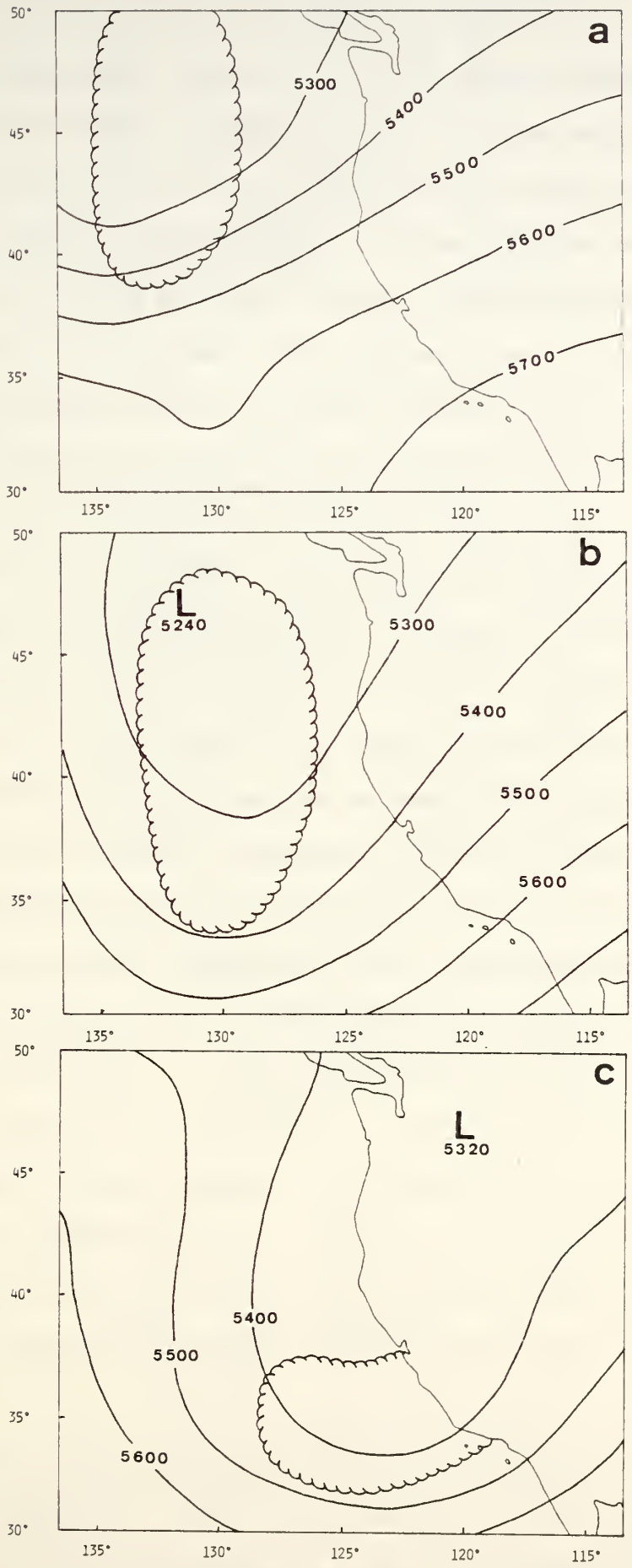

Figure 4. 500 mb height (m) and patchy convective area (scalloped) on: (a) 00GMT 17 Dec 1978; (b) 00GMT 18 Dec; and (c) 00GMT 19 Dec.

charts are shown in Figs. 5a-c. At the initial time (Fig. 5a), the convective area tends to be under the region of maximum cyclonic vorticity. Thus, some of the area is experiencing positive vorticity advection and other parts of the area have negative vorticity advection aloft. Similar comments apply for the southern portion of the convective area in Fig. 5b, whereas the northern portion appears to be in the left front quadrant of a vorticity maximum. As the relative vorticity pattern takes on a crescent-shape (Fig. 5c), the patchy convection area tends to be on the inner (cyclonic) side of the vorticity maximum.

The convective area tends to be found downstream from the 700 mb thermal trough in a region of cold advection (Fig. 6). Thus, the convective towers are building into the cold unstable air aloft. The upper level environment of the convection region is relatively dry, as expected in a polar outbreak. Neither the kinematic nor the normal mode vertical motion fields (not shown) have a consistent relationship with the convection area, which might be expected from the vorticity advection and temperature advection fields indicated in Figs. 5 and 6. However, there is a good relationship between the convective area and the static stability in the lower troposphere. The field of $-\Delta\theta/\Delta p$ between 850 and 700 mb is shown in Fig. 7. The convection is found in regions in which the lapse rate is nearly dry adiabatic. This lapse rate is consistent with the 700 mb cold advection (Fig. 6) above a near surface layer which is warm because of the surface heat flux from the ocean. Notice that there is also low static stability air over the adjacent land area in Fig. 7c, and that the convection over the ocean seems to lead into that area.

To summarize these synoptic relationships, the convective area appears within a cold, dry air flow behind the front. The surface heat and moisture

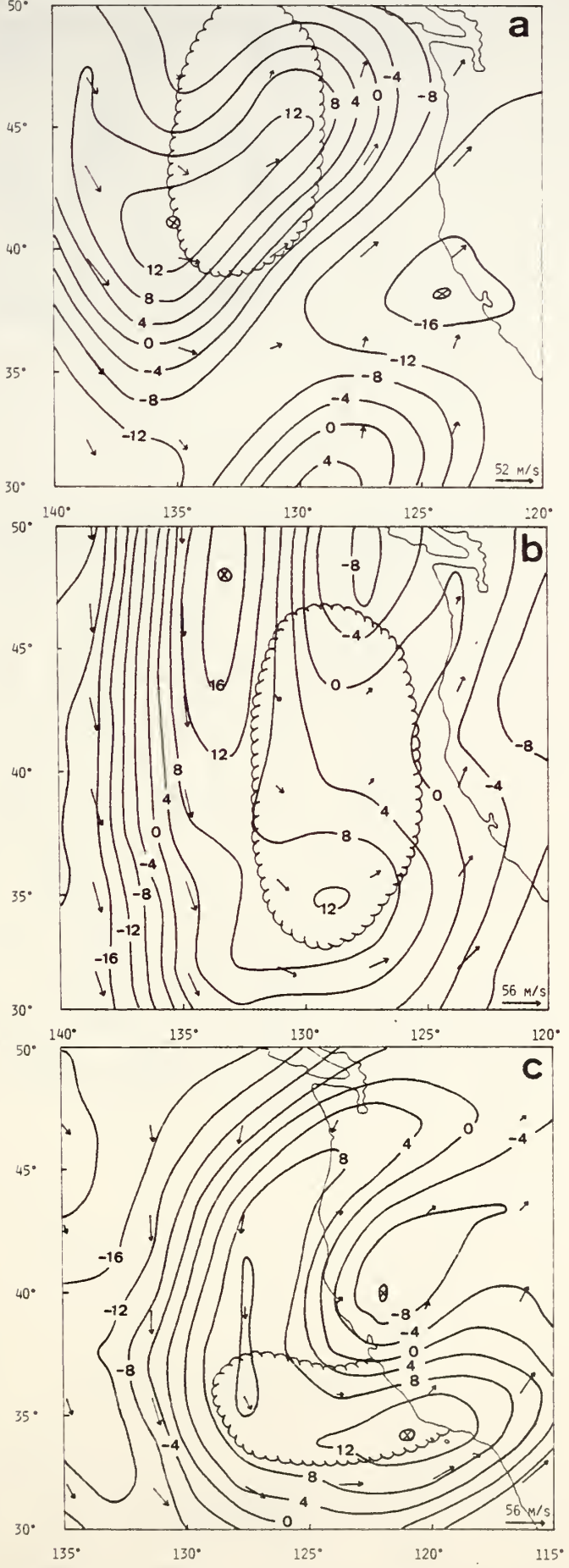

Figure 5. 500 mb relative vorticity (10^{-5} sec^{-1}) and patchy convective area (scalloped) on: (a) 00GMT 17 Dec 78; (b) 00GMT 18 Dec 78; and (c) 00GMT 19 Dec 78. Centers of vorticity are indicated by x and wind vectors are indicated at 3.75° Lat. and Long. according to scale indicated in lower right corner.

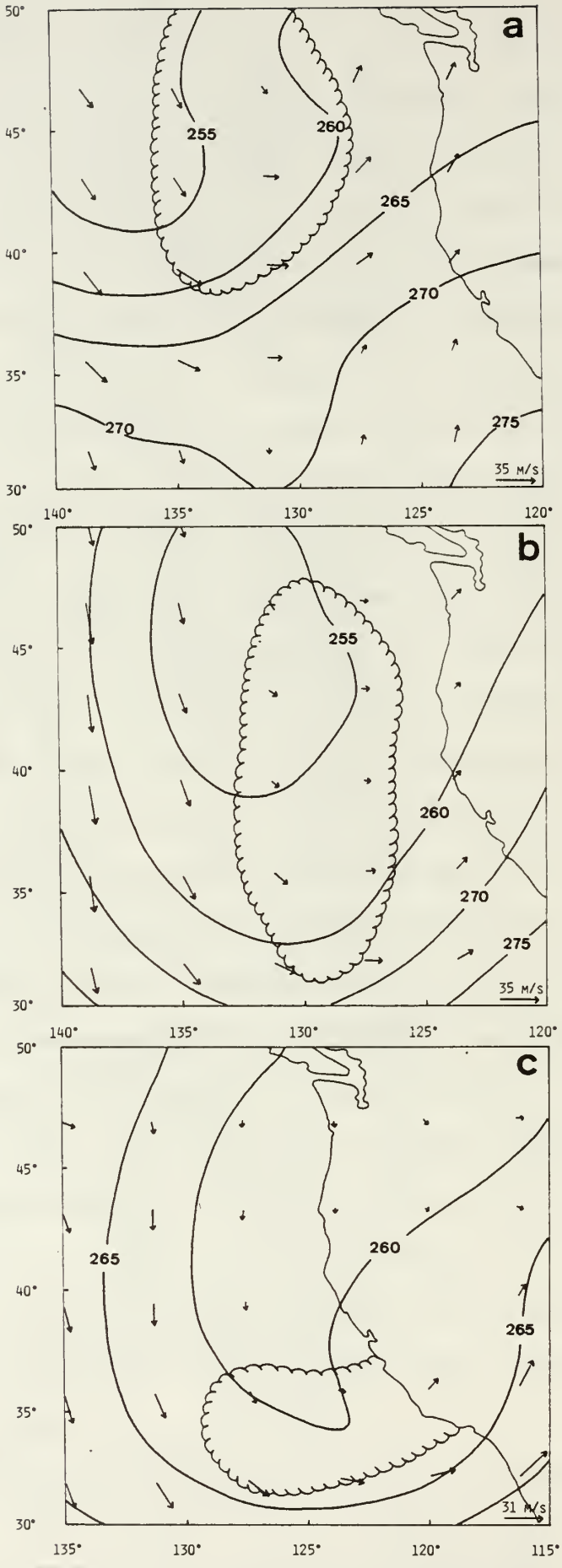

Figure 6. 700 mb temperature (^{o}K) relative to the patchy convection area o
(a) 00GMT 17 Dec 78; (b) 00GMT 18 Dec 78; and (c) 00GMT 19 Dec 7
Wind vectors are indicated at 3.75^{o} Lat. and Long. according to
scale indicated in lower right corner.

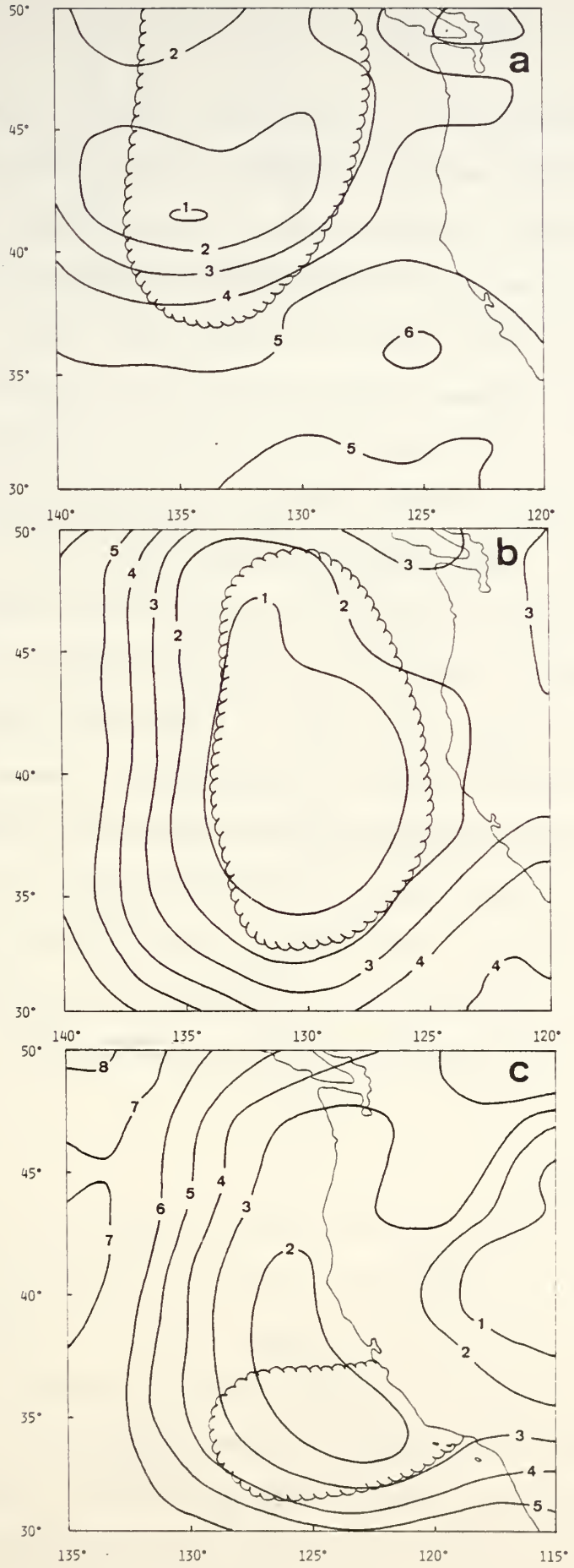

Figure 7. Static stability ($-\Delta\theta/\Delta p$) in the 850-700 mb layer ($^{o}C/100$ mb) relative to patchy convective area (scalloped) on: (a) 00GMT 17 Dec 78; (b) 00GMT 18 Dec 78; and (c) 00GMT 19 Dec.

fluxes from the ocean appear to be the primary driving forces, rather than synoptic scale lifting patterns associated with positive vorticity advection or warm advection aloft. There appears to be destabilization of the convective column due to the cold advection aloft, and perhaps also to upward vertical motion in some areas ahead of the upper level trough.

The NOGAPS-diagnosed cumulus precipitation at 00GMT during the period are shown in Fig. 8. The patchy convective area corresponds very well with this field, especially in view of the fact that this patchy area was over the data-sparse ocean. In the first two periods (Figs. 8a-b), when the patch was very large and located off the coast of Washington and Oregon, the correspondence with the computed precipitation is very remarkable. It is important that the parameterization technique is able to diagnose the areal extent and give some indication of the intensity of the convection. However, this does not necessarily mean that the parameterization scheme will correctly maintain this relationship in a forecast mode (personal communication, Dr. T. Rosmond, NEPRF). If the vertical redistribution of heat, moisture and momentum by the parameterization technique tends to eliminate the relationship with the synoptic fields, the forecasts after a few hours will not reflect the convective area.

b. Case Study 2

This is the first of four other cases that will be briefly described to illustrate the common features associated with moderate post-frontal convection off the California coast. Rather than show an evolution of each case, a single time has been chosen when the convective pattern was well developed.

This example includes a convective patch offshore and another band crossing the coastline at 00GMT 21 Feb 1979 (Fig. 9a). These features are in the cold air behind a major frontal band that is associated with a large-scale

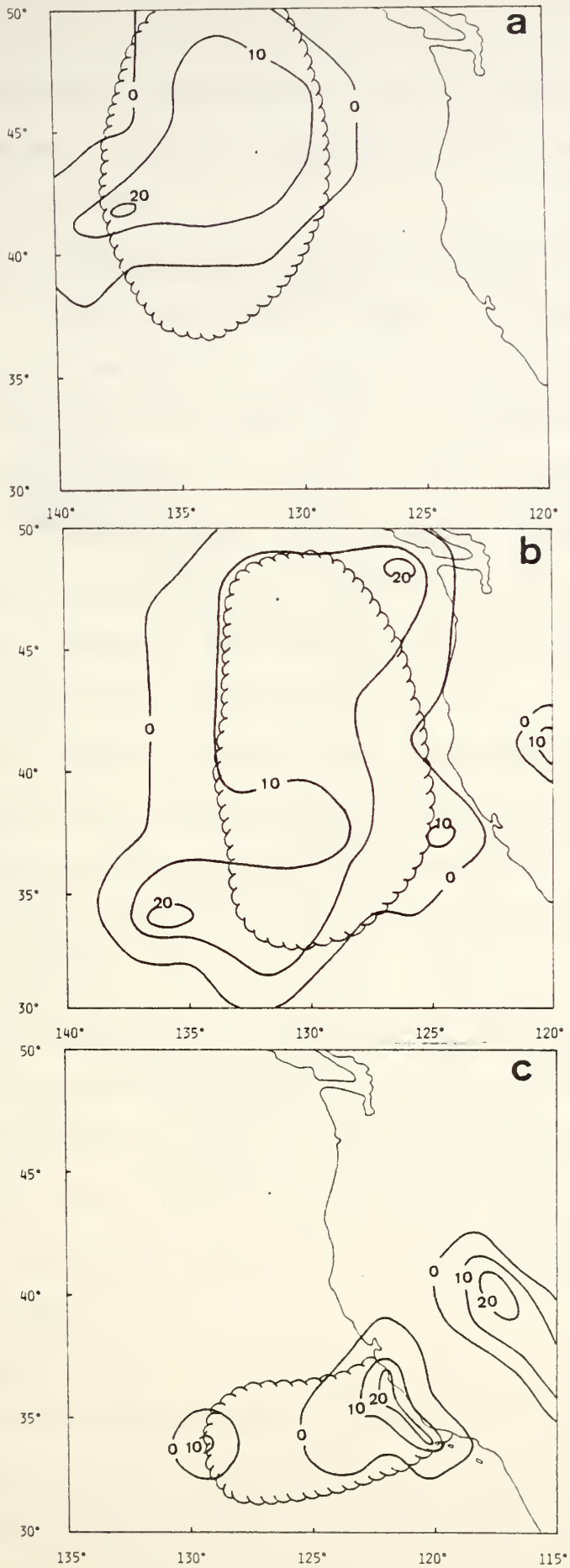

Figure 8. Cumulus precipitation (mm/day) diagnosed from the NOGAPS heating package relative to the patchy convective area (scalloped) on: (a) 00GMT 17 Dec 78; (b) 00GMT 18 Dec 78; and (c) 00GMT 19 Dec 78.

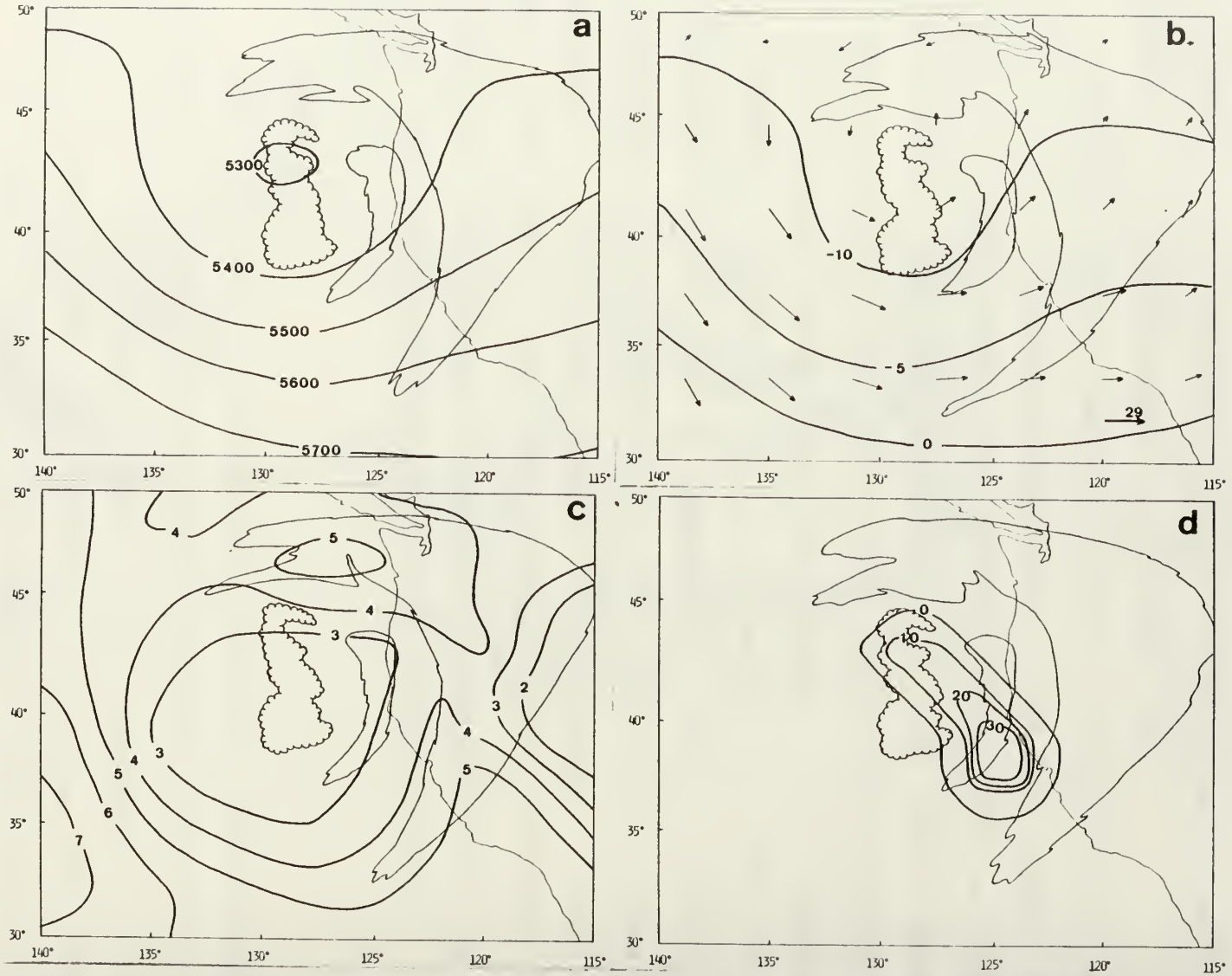

Figure 9. Convective pattern (scalloped) and large scale cloudiness (dashed) on 00GMT 21 February 1979 relative to: (a) 500 mb height (m); (b) 700 mb temperature (°K) and wind vectors at 3.75 lat. and long. according to scale indicated in lower right corner;

trough in the westerlies. The convective patch is located very near the 500 mb low center, whereas the band is farther east in a region of positive vorticity advection (not shown).

The 700 mb temperature field (Fig. 9b) indicates that the thermal trough is nearly in phase with the 500 mb trough. In fact, there is a surface low almost directly below the 500 mb center. Consequently, the convective patch is also near the surface pressure center (not shown) and extends southward along the trough. Whereas the convective patch tends to be located in the coldest air at 700 mb, the band is in a region of cold advection between the thermal trough and the downstream thermal ridge. Most of the large-scale cloud band is in the region of warm advection farther downstream, as would be expected from synoptic scale considerations.

As shown in Fig. 9c, the large-scale trough region is a region of minimum static stability in the 850-700 mb layer. Both the convective patch and the band are contained within the $3^{\circ}C/100$ mb isoline. By contrast, the large-scale cloud band tends to be located in the regions with more stable lower tropospheric air.

The cumulus convection which is diagnosed from the NOGAPS parameterization scheme based on the ECMWF fields is illustrated in Fig. 9d. Rather than indicating two separate convection areas, the cumulus precipitation extends diagonally between the patch and the band. Given the grid size in the ECMWF fields, it is probably unrealistic to expect a distinction between the two convective areas.

c. Case Study 3

The convective patch in 00GMT 31 January 1979 was again embedded in the 500 mb trough (Fig. 10a). As in the previous example, the large-scale cloud band extended westward around the northern side of the 500 mb low. The

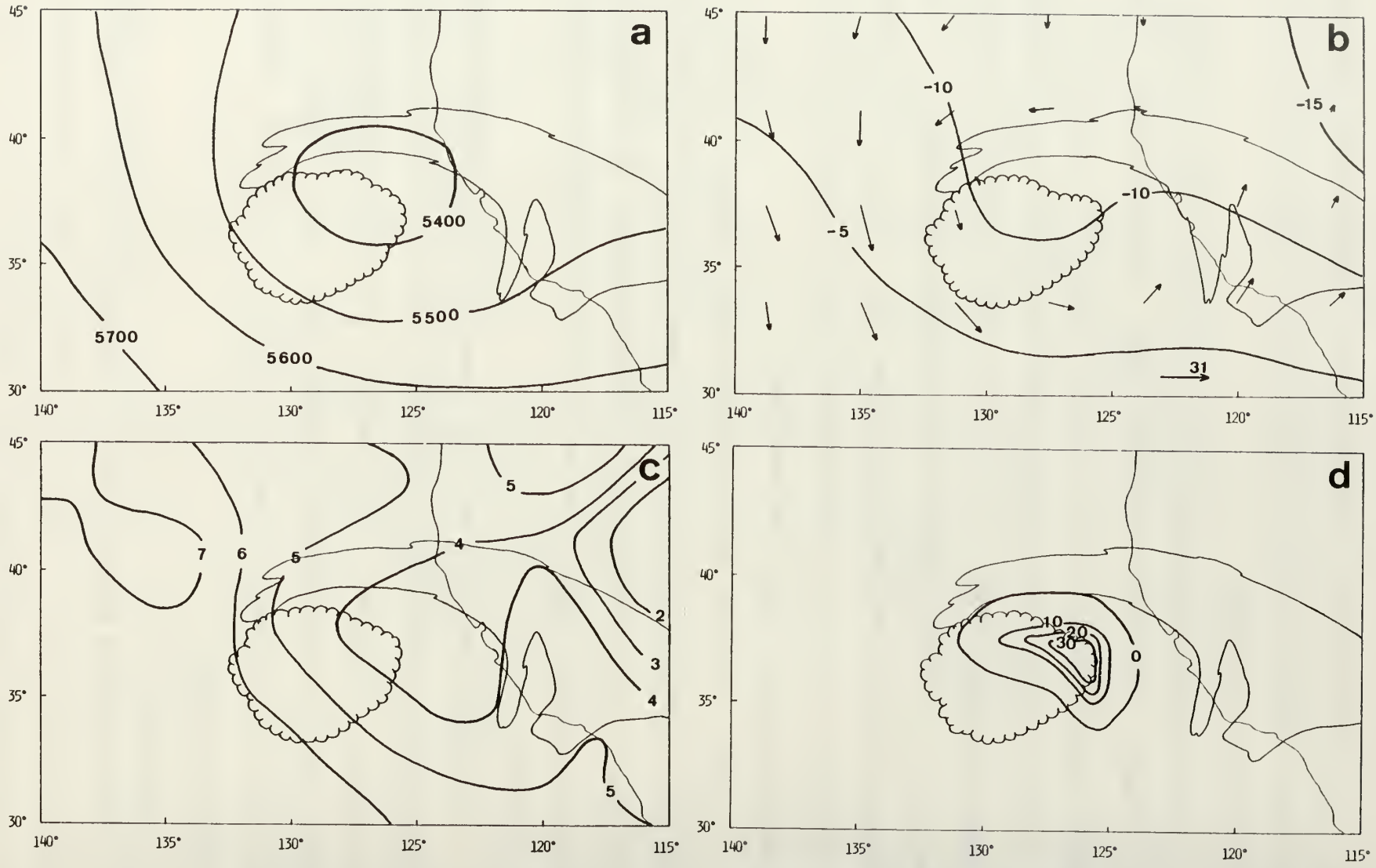

Figure 10. Similar to Fig. 9, except for 00GMT 31 January 1979.

700 mb thermal trough (Fig. 10b) was again nearly directly below the 500 mb trough, so that the surface low (not shown) and 500 mb center were vertically stacked. The convective patch is found in the coldest air and in the cold advection ahead of the thermal trough at 700 mb. By contrast, the large-scale cloud band is found in the warm advection region. The relationship between the convective patch and the 850-700 mb static stability is slightly different in this case. Rather than being embedded within the least stable air, which is just off the California coast, the convective patch appears to be in the gradient region between minimum stability and maximum stability farther upstream. Finally, the location of the diagnosed cumulus convection agrees fairly well with the convective patch (Fig. 10d).

d. Case Study 4

An extensive convective area is found in the region of the 500 mb troughline on 00GMT 16 January 1979 (Fig. 11a). By this time, the frontal band has penetrated to the California-Mexico border. As in the previous cases, the post-frontal convection tends to be found within and in advance of the 700 mb thermal trough (Fig. 11b). There is again excellent agreement between the convection region and the minimum 850-700 mb static stability (Fig. 11c). All of the convection is found within the region of 1-3^{o}C/100 mb values of static stability. Excellent agreement is also found between the convective region and the diagnosed cumulus precipitation field (Fig. 11d).

e. Case Study 5

A band of weak convection extends toward the northwest from a convective patch near 30^{o}N, 123^{o}W on 00GMT 5 January 1979. As indicated in Fig. 12a, this convection is aligned with a northwest-southeast oriented 500 mb trough. A large-scale cloud band is found near the ridge line to the east and northeast. The 700 mb temperature field (Fig. 12b) illustrates that the convective

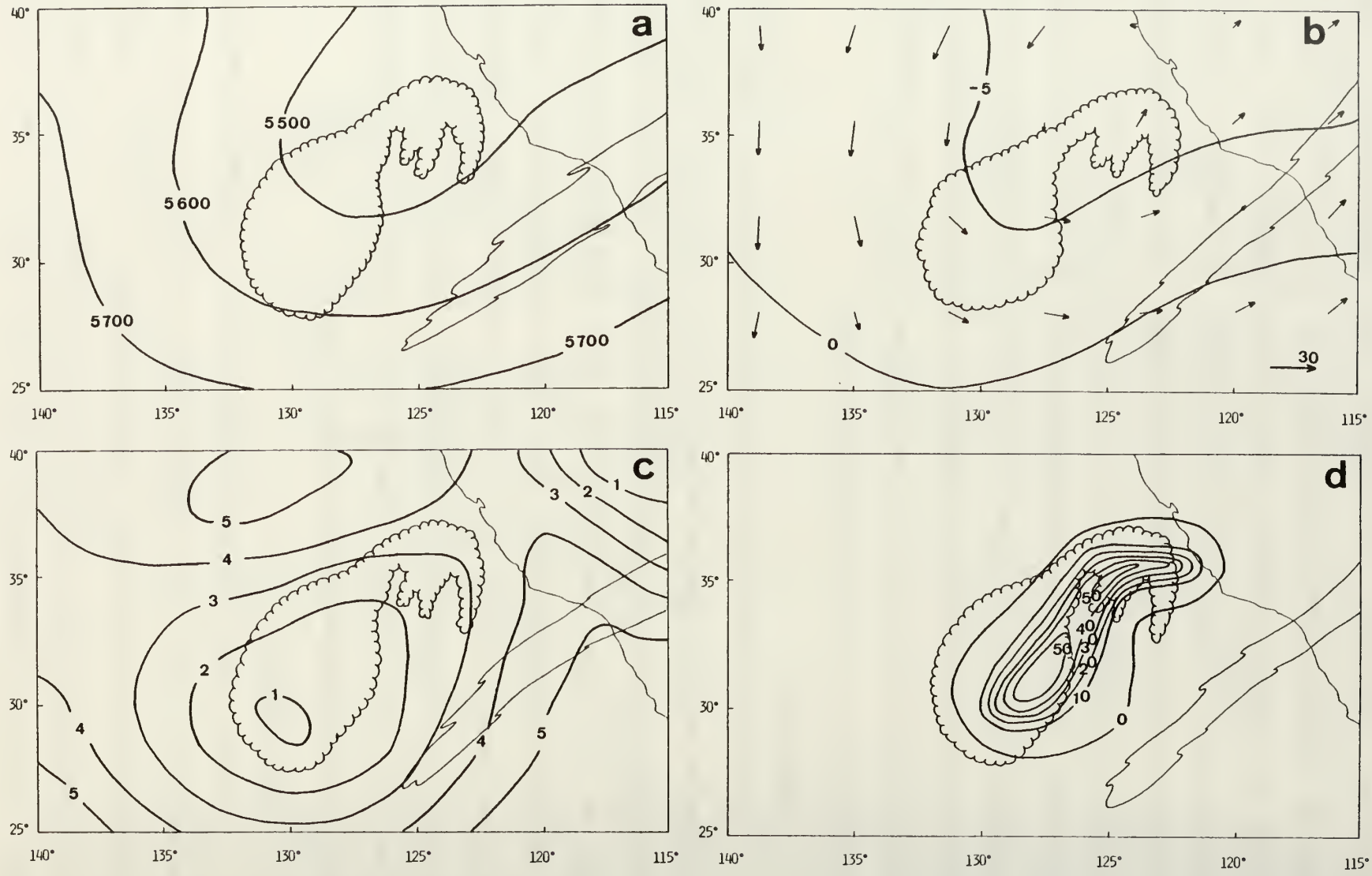

Figure 11. Similar to Fig. 9, except for 00GMT 16 January 1979.

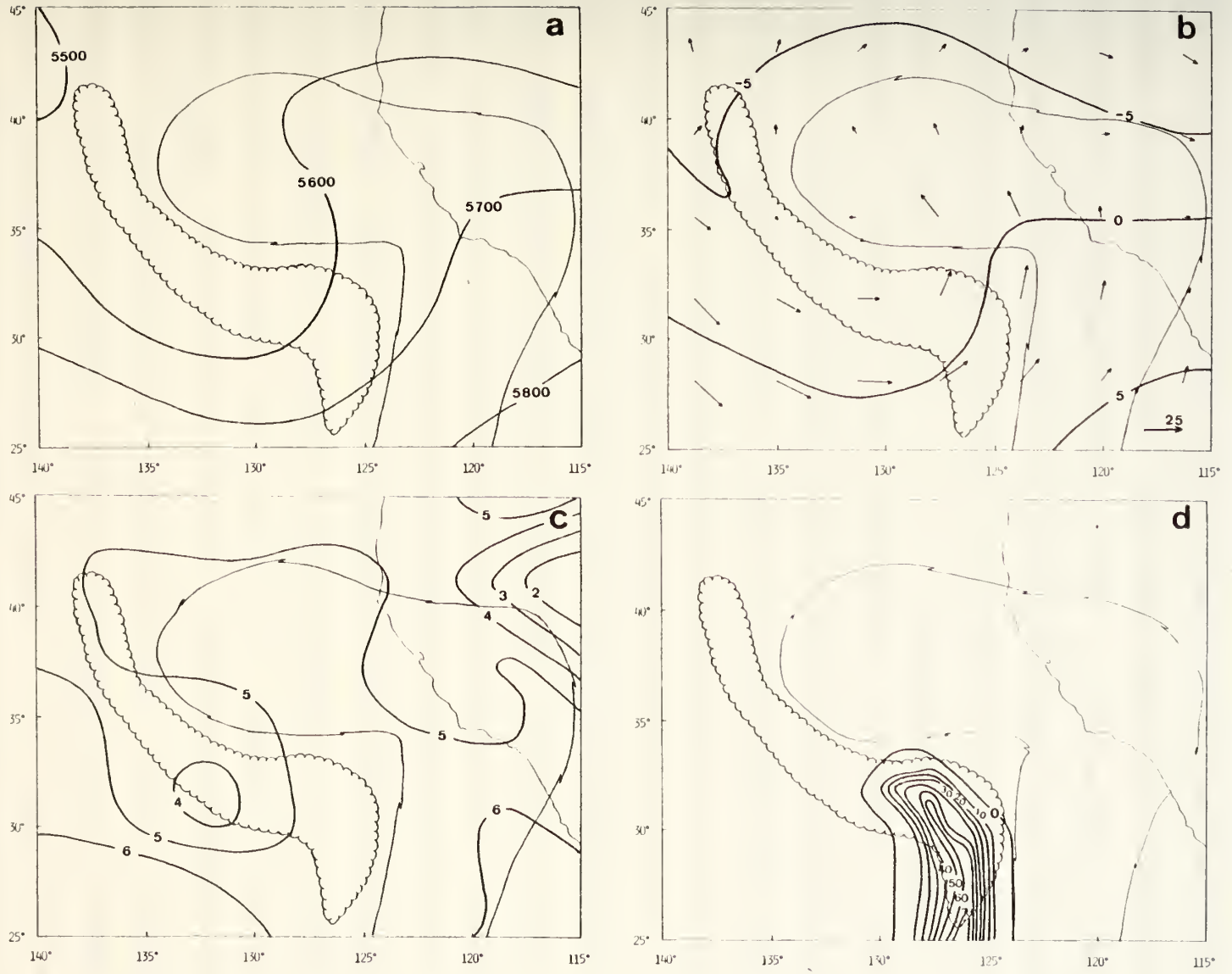

Figure 12. Similar to Fig. 9, except for 00GMT 5 January 1979.

band is within and in advance of the thermal trough, whereas the large-scale band is in the warm advection region. There are also differences in static stability (Fig. 12c) associated with the two cloud regions. The convective band and patch are found along the axis of minimum static stability, whereas the large-scale cloud band tends to be in more stable air. The diagnosed cumulus precipitation (Fig. 12d) agrees fairly well with the location of the convective patch near 30^{o}N, although the precipitation extends too far to the south. There is no indication of the weak cloud band to the northwest.

5. Summary and Conclusions

A five-year series of wintertime synoptic and mesoscale convective situations behind cold fronts off the west coast of North America has been catalogued. The convective situations were classified using the 500 mb and surface patterns and the satellite IR pictures. Several degrees of organization of convective weather have been observed in this study. These included widely scattered cellular convection bands, patches, clusters and commas. An average of about 13 convective events occurs each winter, and two of these cases are likely to have intense and well-organized convection as they cross the coast.

Five cases during the Special Observing Period of FGGE were selected for quantitative study using the ECMWF Level III-B analyses. In each of the five FGGE cases, the post-frontal convective regions were associated with a vertically-stacked surface to 500 mb low located off the West Coast. It is not clear whether the convection contributed to the presence of the surface low by heating the column. It is also possible that the convection is a consequence of the processes leading to a cutoff low. At this stage of the development, the convection is located within the upper level trough and not in the positive vorticity advection region. However, there was one case with a

convective band under the positive vorticity advection aloft and a convective patch in the region of the trough.

The convection was normally found within or in advance of the 700 mb thermal trough. Thus, the air at 700 mb is either already at minimum temperature or is becoming colder with time. This is also consistent with the convection being found in regions of minimum 850-700 mb static stability. That is, the column is being destabilized by cold advection aloft while the surface air is being warmed as it is advected toward the south over higher sea-surface temperatures. In most of the five cases, the potential temperature gradient between these two levels was about $2^{\circ}C/100$ mb, which is approaching a neutral lapse rate. By contrast, the large-scale clouds tended to be found in regions with temperature gradients 2-3 times as large. It should be noted that these are only instantaneous correlations of convection with regions of minimum static stability. These correlations do not indicate cause or effect.

One of the most interesting aspects of this study was the demonstration that the Arakawa-Schubert latent heat parameterization scheme in the NOGAPS provided a relatively good indication of the convective areas. The diagnosed cumulus precipitation areas did not agree exactly with the satellite-observed convective regions. Nevertheless, the agreement was encouraging considering the grid size of the ECMWF fields and the sparsity of data over the oceans.

Diagnostic use of the NOGAPS parameterization as in this study only suggests the <u>potential</u> for prediction of the post-frontal convective areas. When a convective region is indicated by the parameterization technique, a vertical flux of heat, moisture and momentum occurs in a <u>prediction</u> model. If these fluxes rapidly eliminate the conditions necessary for sustaining the convection, and these conditions are not restored by the large-scale forcing, cumulus precipitation will not be continued. In fact, these post-frontal

precipitation regions are frequently not predicted by NOGAPS (Dr. T. Rosmond, personal communication) or other models. Therefore, these tests suggest that there is definitely a potential for improved forecasts of post-frontal convective regions off the West Coast.

Acknowledgments. This research was supported by the National Aeronautics and Space Administration under Contract 623-GW-86B and the Naval Environmental Prediction Research Facility under Program Element 62759N, Project WF59-551, "Numerical Modeling of Unique Tropical Phenomena". Chuck Wash and Jim Peak provided very helpful comments on an earlier version of the manuscript, which was typed by Ms. Marion Marks. The figures were drafted by Ms. Kyong Lee. Jim Boyle gave us valuable assistance in reading the ECMWF tapes, which were provided by Waymon Baker of NASA. The computations were done at the Church Computer Center of the Naval Postgraduate School.

APPENDIX A

Table I. Tabulation of Convective Situations

1977 - 1978 Date	Winter Type	1978-1979 Date	Winter Type	1979-1980 Date	Winter Type
Nov 4-6	Light	Nov 12	Light	Nov 3-4	Light
Dec 18	Light	Nov 21-24	Intense	Jan 15	Light
Dec 23-28	Intense	Dec 17-10	Light	Feb 14-15	Moderate
Jan 10	Moderate	Jan 4-6	Moderate	Feb 17	Moderate
Jan 19	Light	Jan 15-17	Moderate	Feb 19	Moderate
Feb 5-6	Light	Jan 30-Feb 1	Moderate	Feb 21	Moderate
Feb 10-11	Moderate	Feb 21-22	Moderate	Mar 3	Moderate
Feb 13	Moderate	Mar 1	Light	Mar 6-7	Light
Mar 1	Moderate	Mar 15-16	Moderate	Mar 8-10	Light
Mar 4-5	Light	Mar 20-21	Moderate	Mar 21	Light
Mar 9-10	Light	Mar 27-29	Intense	Mar 26	Moderate
Mar 11-12	Moderate	Apr 23-24	Light	Apr 5	Moderate
Mar 21-22	Light			Apr 21-22	Moderate
Mar 31-Apr 1	Moderate			Apr 28-29 1980	Light
Apr 7	Moderate				
Apr 16	Light				
Apr 25-26	Light				

1980 - 1981 Date	Winter Type	1981 - 1982 Date	Winter Type
Dec 5	Light	Nov 24-29	Intense
Jan 23-24	Light	Jan 2	Moderate
Jan 28-30	Intense	Jan 5	Light
Feb 24-25	Moderate	Jan 19-21	Intense
Feb 28-Mar 2	Intense	Jan 27	Light
Mar 5-6	Intense	Jan 28-29	Moderate
Mar 13	Light	Mar 11-12	Light
Mar 20	Moderate	Mar 14-15	Light
Apr 18-20	Light	Mar 16-18	Moderate
		Mar 28-29	Moderate
		Mar 31-Apr 1	Intense
		Apr 7	Light

References

Arakawa, A., and V. R. Lamb, 1977: Computational design of the basic dynamical processes of the UCLA general circulation model. Methods in Computational Physics, 17, Academic Press, 174-265, 337 pp.

Bjorheim, K., et al, 1982: The Global Weather Experiment, Daily Global Analyses, Dec 1978-Feb 1979, European Centre for Medium Range Weather Forecasts, Shinfield Park, England.

Krishnamurti, T. N., 1968: A diagnostic balance model for studies of weather systems of low and high latitudes, Rossby number less than 1. Monthly Weather Review, 96, 197-207.

Lindzen, R. S., 1974: Wave-CISK in the tropics. Journal of Atmospheric Sciences, 31, 156-179.

Locatelli, J. D., P. V. Hobbs, and J. A. Werth, 1982: Meso-scale structures of vortices in polar air streams. Monthly Weather Review, 110, 1417-1433.

Lord, S., 1978: Development and observational verification of a cumulus cloud parameterization. Ph.D. thesis, University of California at Los Angeles.

Mak, M.-K., 1982: On the moist-geostrophic instability. Journal of Atmospheric Sciences, 39, 2028-2037.

Monteverdi, J. P., 1976: The single air mass disturbance and precipitation characteristics at San Francisco. Monthly Weather Review, 104, 1289-1296.

Mullen, S., 1979: An investigation of small synoptic-scale cyclones in polar air streams. Monthly Weather Review, 107, 1636-1647.

Mullen, S., 1982: Cyclone development in polar air streams over the winter time continent. Monthly Weather Review, 110, 1664-1676.

Rasmussen, E., 1979: The polar low as an extratropical CISK disturbance. Quarterly Journal of the Royal Meteorological Society, 105, 531-549.

Reed, R. J., 1979: Cyclogenesis in polar air streams. Monthly Weather Review, 107, 38-52.

Sandgathe, S., 1981: A numerical study of the role of air-sea fluxes in extra-tropical cyclogenesis. Ph.D. thesis, Naval Postgraduate School, 134 pp.

Sanders, F., and J. R. Gyakum, 1980: Synoptic-dynamic climatology of the "bomb". Monthly Weather Review, 108, 1589-1606.

Sardie, J. M., and T. T. Warner, 1983: On the mechanism for the development of polar lows. Journal of Atmospheric Sciences, 40, 869-881.

Staley, D. O., and R. L. Gall, 1977: On the wavelength of maximum baroclinic instability. Journal of Atmospheric Sciences, 34, 1679-1688.

DISTRIBUTION LIST

		No. Copies
1.	Defense Technical Information Center Cameron Station Alexandria, Virginia 22314	2
2.	Library, Code 0142 Naval Postgraduate School Monterey, California 93940	2
3.	Department of Meteorology Library Code 63, Naval Postgraduage School Monterey, California 93940	1
4.	Dr. Russell L. Elsberry, Code 63Es Naval Postgraduate School Monterey, California 93940	7
5.	Mr. James E. Peak, Code 63Pj Naval Postgraduate School Monterey, California 93940	3
6.	Chairman, Department of Meteorology California State University San Jose, California 95192	1
7.	Chairman, Department of Meteorology Massachusetts Institute of Technology Cambridge, Massachusetts 02139	1
8.	Chairman, Department of Meteorology Pennsylvania State University 503 Deike Building University Park, Pennsylvania 16802	1
9.	Chief, Marine and Earth Sciences Library NOAA, Department of Commerce Rockville, Maryland 20852	1
10.	Chief of Naval Operations (OP-952) Navy Department Washington, D.C. 20350	1
11.	Commander Naval Air Systems Command AIR-370 Washington, D.C. 20361	1
12.	Commander Naval Air Systems Command AIR-553 Washington, D.C. 20360	1

13. Commander 1
Naval Oceanography Command
NSTL Station
Bay St Louis, Mississippi 39529

14. Commanding Officer 1
Fleet Numerical Oceanography Center
Monterey, California 93940

15. Commanding Officer 1
Naval Eastern Oceanography Center
McAdie Bldg (U-117)
Naval Air Station
Norfolk, Virginia 23511

16. Commanding Officer 1
U.S. Naval Oceanography Command Center
Box 12, COMNAVMARIANAS
FPO San Francisco 96630

17. Commanding Officer 1
Naval Research Laboratory
ATTN: Library, Code 2620
Washington, D.C. 20390

18. Commanding Officer 1
Naval Western Oceanography Center
Box 113
Pearl Harbor, Hawaii 96860

19. Department of Atmospheric Sciences 1
ATTN: Librarian
Colorado State University
Fort Collins, Colorado 80521

20. Department of Atmospheric Sciences 1
University of Washington
Seattle, Washington 98195

21. Department of Meteorology 1
University of Hawaii
2525 Correa Road
Honolulu, Hawaii 96822

22. Department of Oceanography, Code 68 1
Naval Postgraduate School
Monterey, California 93940

23. Director 1
Atlantic Oceanographic and Meteorology Labs.
15 Rickenbacker Causeway
Virginia Key
Miami, Florida 33149

24. Mr. Mike Fiorino 1
Naval Environmental Prediction
Research Facility
Monterey, California 93940

25. CDR E. J. Harrison, Jr. 1
Fleet Numerical Oceanography
Center
Monterey, California 93940

26. Dr. Ted Tsui 1
Naval Environmental Prediction
Research Facility
Monterey, California 93940

27. Office of Research Administration (Code 012A) 1
Naval Postgraduate School
Monterey, California 93940

28. Superintendent 1
Library Acquisitions
U.S. Naval Academy
Annapolis, Maryland 21402